

Electronic Supplementary Information (ESI) for

# MnOOH nanorods as high-performance anode for sodium ion batteries

Lianyi Shao, Qing Zhao and Jun Chen\*

*Key Laboratory of Advanced Energy Materials Chemistry (Ministry of Education), College of Chemistry, Nankai University, Tianjin 300071, China*

*E-mail: chenabc@nankai.edu.cn*

## Experimental section

### Sample preparation

MnOOH was synthesized by a hydrothermal method. In brief,  $\text{KMnO}_4$  (2 mmol) were dissolved in a mixture of deionized water and polyethylene glycol (PEG) 400 at room temperature under stirring for 1 h. After then, the homogeneous solution was transferred into a 100 mL Teflon stainless steel autoclave, sealed and maintained at  $120^\circ\text{C}$  for 12 h. After cooling down to room temperature, the solution with powders was filtered. The filtered powder was washed thoroughly with deionized water and absolute ethanol and dried at  $80^\circ\text{C}$  in vacuum.

### Material characterization

Structure and morphology of the as-prepared samples were characterized by powder X-ray diffraction (XRD, Rigaku MiniFlex600) with Cu  $K\alpha$  radiation, field-emission scanning electron microscopy (SEM, JEOL JSM-7500F), transmission electron microscopy (TEM, Philips Tecnai FEI) and X-ray photoelectron spectroscopy (XPS, Axis Ultra DLD). The conductivity measurement for MnOOH was performed at 4-point probes resistivity measurement system (RTS-8) using thin wafer with the diameter of 13 mm and the thickness of 0.22 mm.

The electrochemical tests were performed with CR2032 coin cells. The working electrode was fabricated by mixing the as-prepared sample, Super P and sodium carboxymethylcellulose (CMC-Na) in the weight ratio of 6:3:1 using deionized water as solvent. Afterwards, the slurry was coated on copper foil and dried at  $80^\circ\text{C}$  for 12 h in vacuum. The electrode film was then cut into discs with a diameter of 10 mm and an average weight of  $0.8 \text{ mg cm}^{-2}$ . The coin cells were assembled in an argon-filled glove box using sodium metal as the counter/reference electrode, glass fiber as the separator and 1 M sodium trifluoromethanesulfonate ( $\text{NaSO}_3\text{CF}_3$ , NaTf) in tetraethylene glycol dimethyl ether (TEGDME) or 1 M sodium perchlorate ( $\text{NaClO}_4$ ) in propylene carbonate (PC) with additive fluoroethylene carbonate (FEC, 5 wt.%) as electrolyte. Galvanostatic charge/discharge tests were performed between 0.005-2.8 V on a LAND battery-test instrument (CT2001A). Cyclic voltammetry (CV) was carried out at room temperature using a Parstat 263A electrochemical workstation (AMETEK). The electrochemical impedance spectroscopy (EIS) measurements were carried out using a Parstat 2273 electrochemical workstation over a frequency range from 0.1 Hz to 100 kHz.

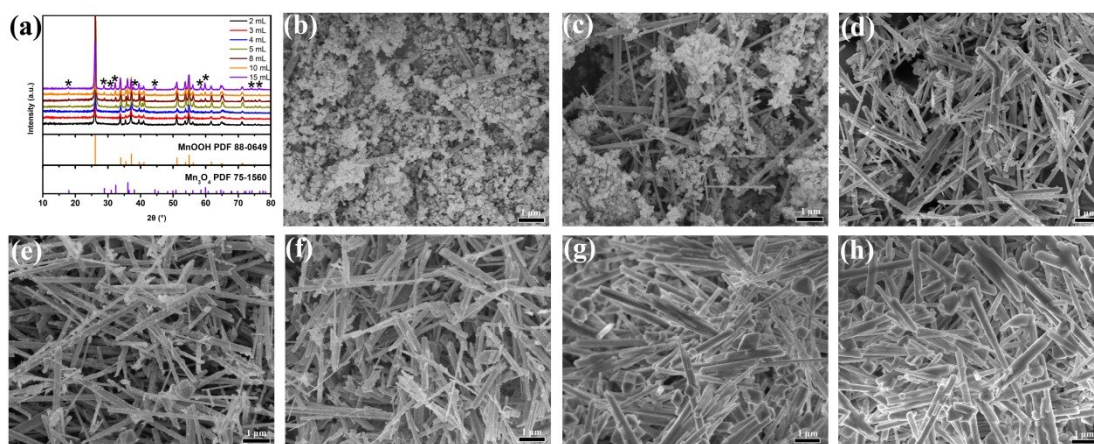


**Fig. S1** (a) XRD patterns of the samples prepared at 120°C for 12 h at different content of PEG 400, the corresponding SEM images of the obtained samples: (b) 2 mL PEG 400, (c) 3 mL PEG 400, (d) 4 mL PEG 400, (e) 5 mL PEG 400, (f) 8 mL PEG 400, (g) 10 mL PEG 400, (h) 15 mL PEG 400.

Fig.S1a shows that the pure MnOOH can be prepared under lower content of PEG 400 (2-4 mL). When increased the dosage of PEG 400, the diffraction peaks of Mn<sub>3</sub>O<sub>4</sub> appear and increase, indicating that the high content of reductant is beneficial to transform MnOOH to Mn<sub>3</sub>O<sub>4</sub>. As shown in Fig.S1b, the products prepared under 2 mL of PEG 400 consist of large quantity of small particles and small amount of nanorods. The amounts of the nanorods increase with the increasing of the content of PEG 400, demonstrating that small particles can gather to form rods. However, further increasing PEG 400 to 5 mL, some irregular bulk morphologies are observed. When the dosage of PEG 400 reached 15 mL, the phenomenon that rods are aggregated together to form irregular bulks is especially obvious. Combined with XRD and SEM results, it should be noticed that the optimal dosage of PEG 400 (4 mL) is favorable for the formation of pure MnOOH nanorods.

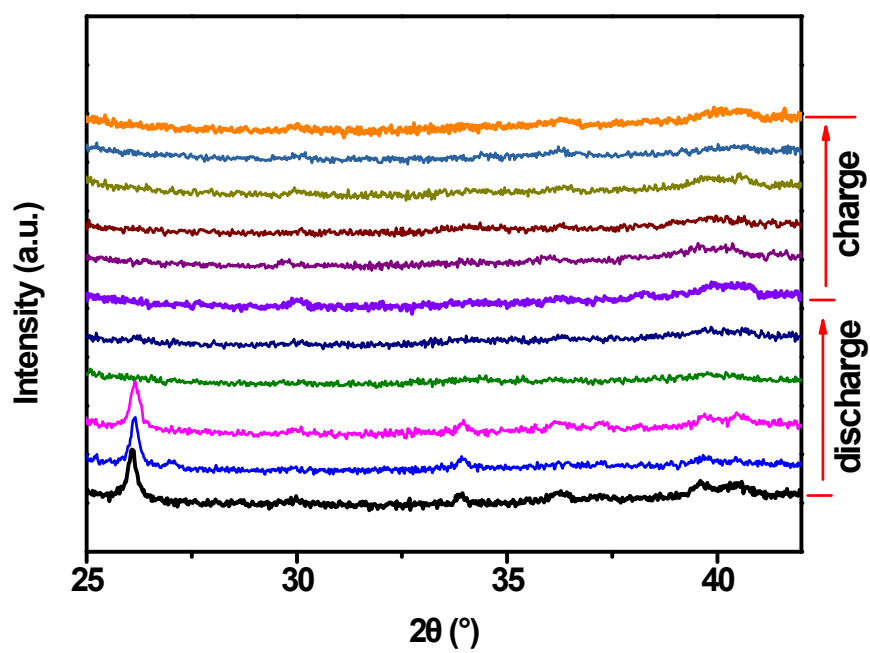


**Fig. S2** Ex-situ XRD patterns of MnOOH electrode during the first cycle at the current density of  $40 \text{ mA g}^{-1}$ .

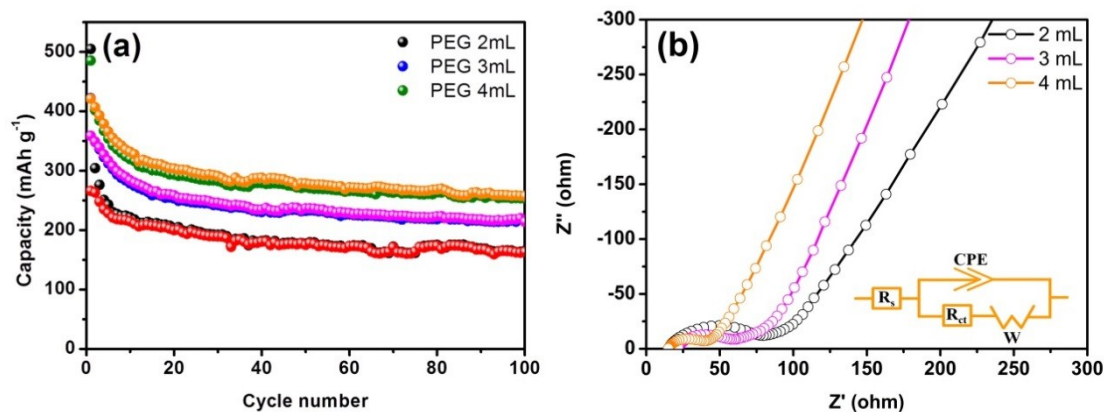


**Fig. S3** (a) cycling properties of MnOOH electrodes at the current density of  $80 \text{ mA g}^{-1}$  in different dosage of reductant, (b) the corresponding EIS curves of MnOOH electrodes in different dosage of reductant.

Fig.S3a shows that the cycling properties of MnOOH are enhanced with the increase of the dosage of reductant. In addition, the electrochemical impedance spectra contain one semicircle in the high frequency region and a line in the low frequency region, corresponding to charge transfer resistance ( $R_{ct}$ ) and Warburg diffusion ( $W$ ). A simplified equivalent circuit inserted in Fig. S3b is used to fit the EIS, which includes the electrolyte and battery component resistance ( $R_s$ ), a constant phase element (CPE) corresponded to the interfacial resistance,  $R_{ct}$  and  $W$ . Obviously, the  $R_{ct}$  of MnOOH electrode (prepared by PEG 4 mL,  $22.14 \Omega$ ) is smaller than that of MnOOH electrode (prepared by PEG 2 mL,  $64.26 \Omega$ ) and that of MnOOH electrode (prepared by PEG 3 mL,  $40.42 \Omega$ ), respectively, revealing that the sample possesses better kinetic property. The results are in accordance with the results of the cycling performance as shown in Fig. S3a.

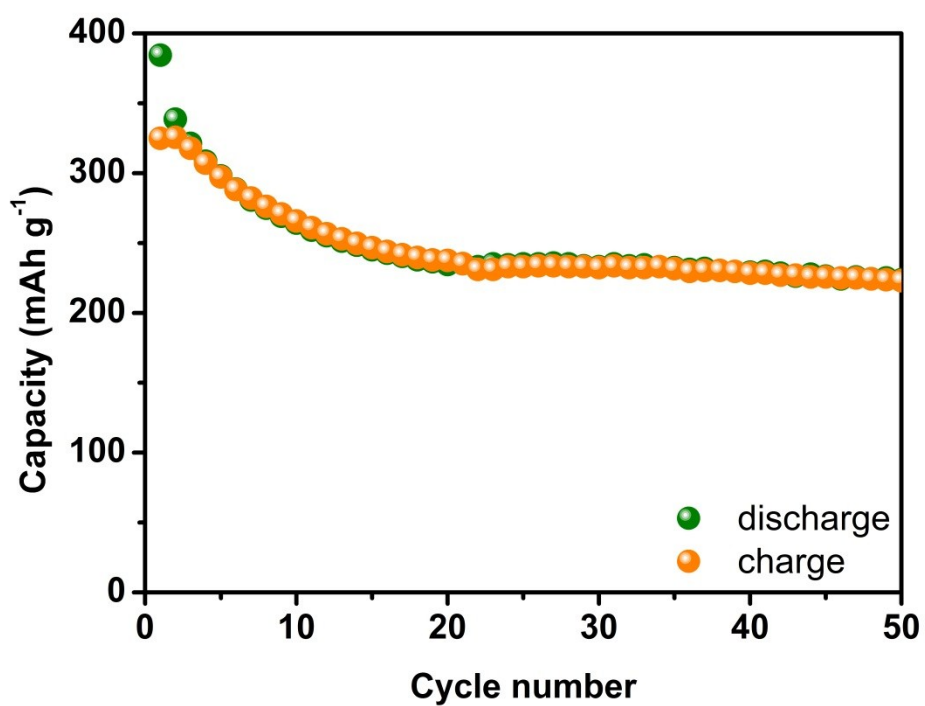


**Fig. S4** Cycling properties of MnOOH at the current density of 500 mA g<sup>-1</sup> in the potential window of 0.005-2.8 V.

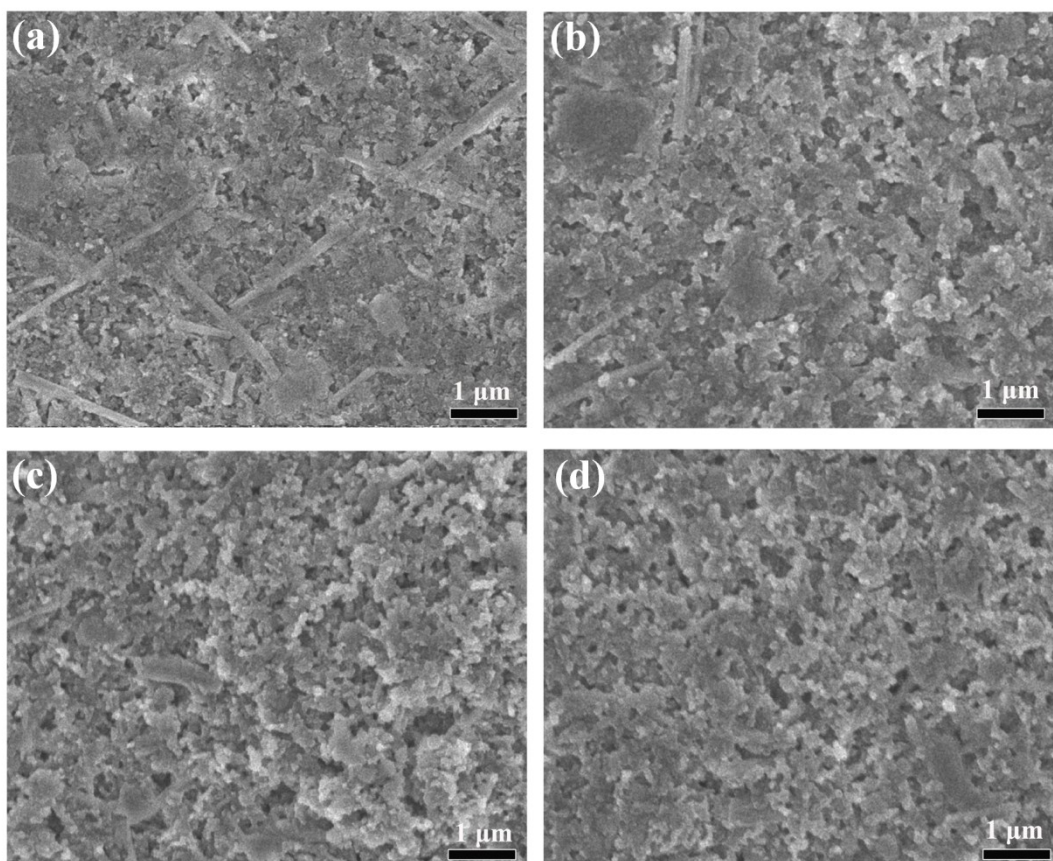


**Fig.S5** SEM images for (a) pristine MnOOH electrode before cycle, (b) MnOOH electrode after the first cycle at the current density of  $80 \text{ mA g}^{-1}$ , (c) MnOOH electrode after 15 cycles at the current density of  $80 \text{ mA g}^{-1}$ , (d) MnOOH electrode after 100 cycles at the current density of  $80 \text{ mA g}^{-1}$ .

Fig.S5a shows the morphology of pristine MnOOH electrode before cycle. Some rods and small super P carbon can be observed. After the first cycle, the rods start to crack into small particles, demonstrating volume strains upon sodium insertion and extraction and the capacity loss. The interconnected particles are the domain morphology of the electrode after 15 cycles. The morphology can be stable in the following 85 cycles. The stable morphology can result in the stable cycling performance. The results are consistent with the electrochemical properties of MnOOH as shown in Fig. 3.

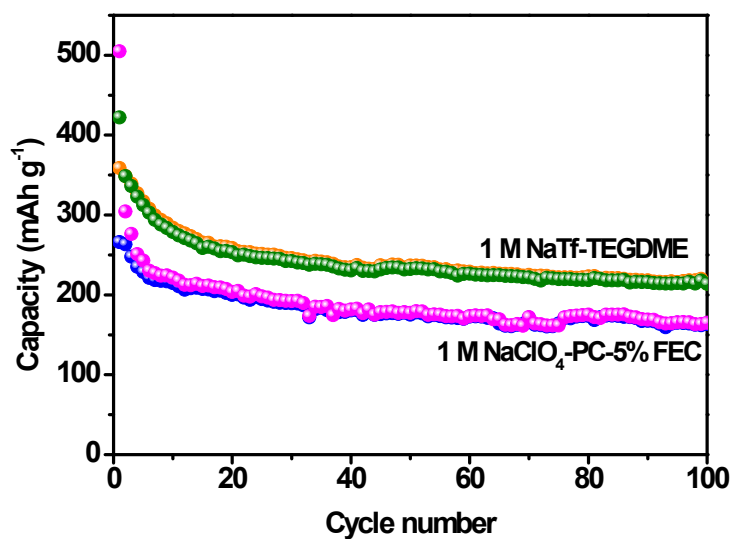


**Fig. S6** Cycling properties of MnOOH at the current density of 80 mA g<sup>-1</sup> in different electrolyte in the potential window of 0.005-2.8 V.

Table S1. Comparison in the redox potential of SIBs anodes.

Material	Redox potential(V)	Potential polarization(V )	Ref.
CuO	0.05/0.5	0.45	1
	0.46/1.85	1.39	
	1.6/2.3	0.7	
NiO	0.8/1.6	0.8	2
Co <sub>3</sub> O <sub>4</sub>	0.54/1.5	0.96	3
FeS	0.24/1.46	1.22,	4
	0.76/1.87	1.11	
Co <sub>9</sub> S <sub>8</sub>	0.6/1.8	1.2	5
ZnS	0.11/0.86	0.75	6
MnOO	0.50/1.03	0.53	This work
H	2.28/2.47	0.19	

## References

- 1 S. Yuan, X. L. Huang, D. L. Ma, H. G. Wang, F. Z. Meng and X. B. Zhang, *Adv. Mater.*, 2014, **26**, 2273.
- 2 F. Zou, Y. M. Chen, K. Liu, Z. Yu, W. Liang, S. M. Bhaway, M. Gao and Y. Zhu, *ACS Nano*, 2016, **10**, 377.
- 3 M. M. Rahman, A. M. Glushenkov, T. Ramireddy and Y. Chen, *Chem. Commun.*, 2014, **50**, 5057.
- 4 S. Y. Lee and Y. C. Kang, *Chemistry*, 2016, **22**, 2769.
- 5 Y. N. Ko and Y. C. Kang, *Carbon*, 2015, **94**, 85.
- 6 D. Su, K. Kretschmer and G. Wang, *Adv. Energy Mater.*, 2016, **6**, 1501785.